

CrossMark
click for updatesCite this: *RSC Adv.*, 2016, 6, 81597

Design of triphenylamine appended anthracene derivatives: electro-polymerization and their electro-chromic behaviour†

Dines Chandra Santra, Sanoy Mondal and Sudip Malik*

Three derivatives (2-TPACNANT, 2,6-TPACNANT and 2,6-TPAANT) of anthracene as a core interior with terminal one or two triphenylamine sides have been designed and synthesized with the aim of obtaining terminal active sites for the purpose of electrochemical polymerization. Electro-deposited polymer films of p-2,6-TPACNANT and p-2,6-TPAANT on ITO/glass electrodes have been obtained within the voltage range from 0 to 1.6 V by repeating cyclic voltammetry (CV) scanning of constant monomer solutions in an electrolyte. The film thickness is easily tuned by controlling the number of the CV scans. Interestingly, these electrogenerated polymer films reveal the reversible electrochemical responses and distinguishable colour changes upon electro-oxidation, which is switched many times by potential modulation. Spectroelectrochemical studies of the electrochromic films on ITO have indicated two colour electrochromism of p-2,6-TPAANT (brick red-dark blue) and p-2,6-TPACNANT (orange-dark blue) with a high colour contrast ratio (ΔT) 87% at 770 nm for p-2,6-TPAANT and 86% at 800 nm for p-2,6-TPACNANT, respectively. These polymer films have the faster response time (1.2–1.3 s) and high colouration efficiency (200–222 cm² C⁻¹). A hand made and simple module has been fabricated in a solidified device composed of the electrodeposited polymers, a pair of ITO electrodes, and a polymer-supported electrolyte to show the potential of using these novel anthracene derivatives as electrochromic materials.

Received 8th June 2016
Accepted 10th August 2016

DOI: 10.1039/c6ra14926j

www.rsc.org/advances

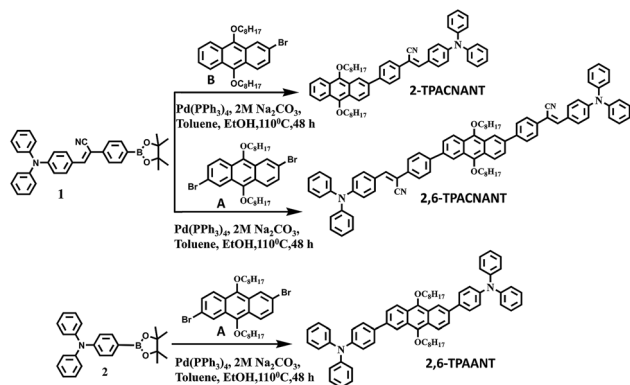
Introduction

Electrochromism is a phenomenon where a material can reversibly change its colour by an electrochemical reaction.¹ Electrochromic materials (ECMs) have received great interest in modern society owing to their potential applications, such as information storage,^{2,3} electrochromic display,^{4,5} optical switch^{6–9} smart windows,^{10,11} and antiglare rear-view mirrors.^{12,13} A typical good electrochromic device must have the criteria such as high colouration efficiency (CE), high optical contrast (ΔT), short response time, good stability, and optical memory, that make them good choice for electrochromic applications.¹⁴ Usually, there are three main types of electrochromic materials: inorganic metal oxides,¹⁵ conducting polymers¹⁶ organic small molecules¹⁷ and their corresponding metal complexes,¹⁸ which have been developed and studied as well.

Liou's and Hsiao's groups reported a few electrochromic materials which were based on polyamides and polyimides consisting of a triphenylamine (TPA) moiety, utilizing its photo-electroactive properties such as hole-transporters, light-emitters, and memory devices.^{19–21} TPA units that are easily oxidized in oxidation process, produce stable radical cations and subsequently a strong change of colouration is observed. Nelson and Adams *et al.* explained that the unsubstituted TPA moieties undergo dimerization (coupling) to tetraphenylbenzidine (TPB) after the formation of a monocation radical.²² After the loss of two protons, the TPB unit is more prone to oxidation as compared to TPA. TPB undergoes further oxidation in two discrete one-electron steps to give TPB^{•+} and finally the quinoidal TPB²⁺.^{22a} It is generally found that electron-donating substituents (such as methoxy groups) stabilize the cation radicals, whereas electron-withdrawing groups (such as the nitro group) have the opposite effect.^{22c} Few triarylamine-terminated monomers have been designed so far to electro-polymerize in different electrolyte solutions. Moreover, π -conjugated polymers have become popular now-a-days as they combine several advantages such as fast response time, high optical contrast ratios, colour tunability, good long-term stability as well as mechanical deformability. The advantage of electrochemical polymerization lies in the smoother coating of the electrode surface directly during the chemical

Polymer Science Unit, Indian Association for the Cultivation of Science, 2A & 2B Raja S. C. Mullick Road, Jadavpur, Kolkata – 700032, West Bengal, India. E-mail: psusm2@iacs.res.in

† Electronic supplementary information (ESI) available: Preparation of three derivatives and their characterization data, polymerization pathway, UV-vis of polymer films, repeated CV scanning of 2-TPACNANT, CV diagram of 1 mM ferrocene, photo of polymer films and IR of polymers. See DOI: 10.1039/c6ra14926j



Scheme 1 Synthesis routes of three derivatives.

polymerization. Attaching electropolymerizable triarylamine units with π -conjugated systems will not only give a chromic monomeric unit, it will also produce electrochromic films with the reversible responses and distinguishable colour changes upon electro-oxidation.

In the present study, three derivatives of 9,10-dialkoxyanthracene have been designed by inserting dialkoxy groups at the 9,10-position of anthracene with the expectation of an enhancement in the solubility in common organic solvents, as well as in the electron density of the anthracene core. TPA appended derivatives at 2 or 2,6-position of 9,10-dialkoxyanthracene have been synthesized (**2-TPACNANT**, **2,6-TPACNANT** and **2,6-TPAANT**; Scheme 1) and their electrochemistry and electro-polymerization have been investigated. It has been found that the single TPA-terminated anthracene derivatives (**2-TPACNANT**) do not undergo electropolymerization, whereas other two derivatives undergo electropolymerization more easily. The presence of two terminal TPA groups has provided a pair of lone electron on the N atom, which has readily led to the electro-polymerization to obtain the corresponding two electrodeposited polymers. The electrochemical and electrochromic properties of the electrodeposited films from the both TPA-terminated anthracene derivatives have also been explored. The experimental results have suggested that the electrodeposited **p-2,6-TPACNANT** and **p-2,6-TPAANT** films revealed reversible electrochemical redox reactions and showed distinguishable colour changes upon electro-oxidation. The spectroelectrochemical behaviour and dynamic electrochromic characterization of the electrodeposited films in solution have mainly been investigated.

Experimental

Materials and instrumentation

2,6-Dibromo-9,10-bis(octyloxy)anthracene (**A**) and 2-bromo-9,10-bis(octyloxy)anthracene (**B**), *N,N*-diphenyl-4-(4,4,5,5-tetramethyl-1,3,2-dioxaborolan-2-yl)aniline (**2**), and 2-[4-(4,4,5,5-tetramethyl-1,3,2-dioxaborolan-2-yl)phenyl]-3-[4-(*N,N*-diphenylamino)phenyl]acrylonitrile (**1**)^{23,24} were synthesized according to the literature procedure. Tetrakis (triphenyl phosphine) palladium (0),

tetrabutyl ammonium perchlorate (Bu_4NClO_4), silver chloride (AgCl), polymethylmethacrylate (PMMA), lithium perchlorate (LiClO_4) *etc.* and solvents (dichloromethane (DCM), methanol (MeOH), acetone (CH_3COCH_3), acetonitrile (CH_3CN) *etc.*) were used as received from the commercial sources. All derivatives were prepared by $\text{Pd}(\text{PPh}_3)_4$ assisted Suzuki coupling reactions in high yield. Detailed synthetic procedures and characterization data were given in the ESI.[†] The synthetic route and chemical structures of three derivatives are illustrated in Scheme 1.

^1H and ^{13}C NMR spectra were measured on a Bruker 400 or 500 MHz FTNMR system with tetramethylsilane (TMS) as an internal standard. Fourier transformed infrared spectra were recorded on a Horiba FT-720 FT-IR spectrometer. HRMS were taken using a Quadrupole-TOF (Q-TOF) micro MS system using an electrospray ionization technique. MALDI-TOF mass spectrometry was carried out with a Bruker Daltonics FLEX-PC. Electrochemistry was performed with a CHI 6087E electrochemical analyzer. Cyclic voltammetry was conducted with the use of a three-electrode cell in which ITO was used as a working electrode, a platinum wire was used as an auxiliary electrode and a home-made Ag/AgCl , KCl (sat.) as the reference electrode. Ferrocene was used as an external reference for calibration (+0.44 V vs. Ag/AgCl). Voltammograms were presented with the positive potential pointing to the left, with increasing anodic currents pointing downwards. Spectroelectrochemistry analyses were carried out with an electrolytic cell, which was composed of a $1 \times 2 \text{ cm}^2$ cuvette, ITO as a working electrode, a platinum wire as an auxiliary electrode, and an Ag/AgCl reference electrode. Absorption spectra in the spectroelectrochemical experiments were measured with an Agilent 8453 UV-visible spectrophotometer.

Results and discussion

2,6-Dibromo-9,10-bis(octyloxy)anthracene (**A**) were reacted separately with compound **1** and **2** in the presence of $\text{Pd}(\text{PPh}_3)_4$ in ethanol–toluene mixture to receive **2,6-TPACNANT** and **2,6-TPAANT** with relatively good yield. **2-TPACNANT** was synthesized from the reaction between 2-bromo-9,10-bis(octyloxy)anthracene (**B**) and compound **1**. Formation and purities of all those derivatives were checked with NMR and MALDI-TOF (Fig. S4–j[†]).

Electrochemical polymerization

Electrochemical polymerization processes of two monomers were performed on the ITO glass slides using a 1 mM monomer solution in 0.1 M $\text{Bu}_4\text{NClO}_4/\text{DCM}$ *via* repetitive cycling between 0 to 2 V at a potential scan rate of 50 mV s^{-1} (Fig. 1). As the CV scan continued, a polymer film was deposited on the working electrode (ITO) surface. With an increase in the number of CV scans, the current densities were increased. It implied the gradual deposition of conducting polymers on the surface of the electrode. The polymerizations of **2,6-TPAANT** (Fig. 1a) produced two oxidation peaks ($E_{1/2} = 0.89 \text{ V}$ and 1.03 V) which were assigned to their two states (i) polaronic and (ii)

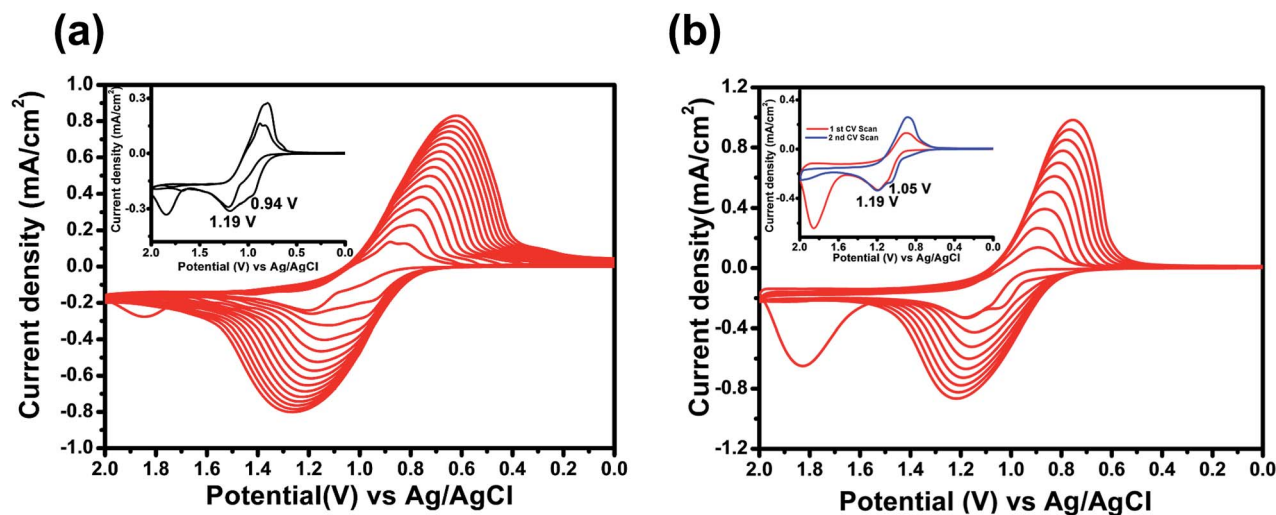


Fig. 1 Repeated CV scanning of (a) 2,6-TPAANT and (b) 2,6-TPACNANT between 0 to 2 V in 0.1 M $\text{Bu}_4\text{NClO}_4/\text{DCM}$ with a scan rate of 50 mV s^{-1} . The inset displays the first and second scans.

bipolaronic states, respectively. However, only one oxidation peak (E^{ox}) was observed at 1.19 V at the first scan and it was recognized to the oxidation of TPA unit (inset of Fig. 1a). During the second scan, a new shoulder like oxidation peak appeared at 0.94 V and the wave was moved to a more positive potential. With increasing current, the peak became broad and also gradually merged after a few CV scans. It indicated that the oxidative coupling between the TPA units produced a tetraphenylbenzidine (TPB) unit with greater extended p-conjugation. As a result, TPB showed a lower oxidation potential than the original TPA unit²⁰ (Scheme S1†).

The electrochemical polymerizations of 2,6-TPACNANT showed similar result as presented in Fig. 1b. In the first scan, only one oxidation peak (E^{ox}) at 1.19 V was attributed to the oxidation of the TPA unit. In the second scan, two oxidation peaks appeared at 1.05 V and 1.19 V, respectively. During the second scan a new shoulder-like oxidation peak appeared at

1.05 V due to the *in situ* formation of the TPB unit during the first CV scan. Significantly, the wave shifted to a more positive potential with increased current densities, indicating that polymerizations of 2,6-TPACNANT were taking place in the solution. It was further supported by the formation of an orange coloured film observed by the naked eye. The two oxidation peaks of 2,6-TPACNANT became indistinguishable into one broad peak after a few CV cycles.

In the successive CV of the compound 2-TPACNANT in the same solution between 0 and 1.6 V, only one oxidation peak (E^{ox}) at 1.28 V in the first scan was observed. A new oxidation wave appeared as a shoulder at 1.15 V related to the presence of the TPB unit. As shown in Fig. S2,† no significant increase in the redox wave current density was observed as the CV scan continued. It was worthy to note that no polymer film was deposited on the electrode surface. Results indicated that the mono-TPA compound seemed to couple to a dimer during the

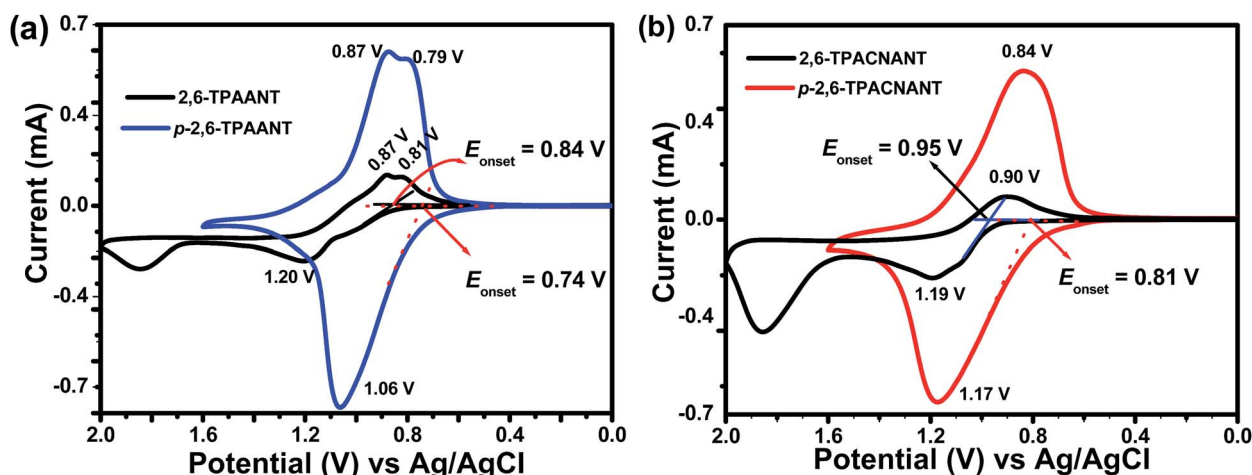


Fig. 2 Cyclic voltammograms of the (a) p-2,6-TPAANT and (b) p-2,6-TPACNANT polymer film deposited on the ITO glass in 0.1 M $\text{Bu}_4\text{NClO}_4/\text{MeCN}$ at a scan rate of 50 mV s^{-1} .

oxidative process. Based on the significant observation, it was proposed that during the electrochemical polymerization, the linear conjugated polymers were formed from the symmetric

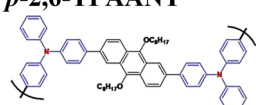
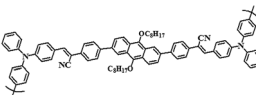
TPA-appended anthracene derivatives as shown in Table 2. In Fig. 3, red-shifting of the absorption maxima as well as the onset of the polymer films as compared to respective

Table 1 Optical and electrochemical properties of monomers and the electrochemically synthesized polymers

Monomers and polymers	Absorption wavelength ^a (nm)		Oxidation potential ^b (V)		E_g^c (eV)	Energy levels ^d (eV)	
	λ_{\max}	λ_{onset}	E_{onset}	$E_{1/2}^{\text{ox}}$		HOMO	LUMO
2,6-TPAANT	360	465	0.84	1.04	2.67	5.43	2.76
p-2,6-TPAANT	376	588	0.74	0.97	2.11	5.36	3.25
2,6-TPACNANT	427	490	0.95	1.05	2.53	5.44	2.91
p-2,6-TPACNANT	436	557	0.81	1.01	2.23	5.40	3.17

^a UV-vis absorption maximum and onset wavelengths for the polymer films. ^b Read from the first CV scans, in acetonitrile at a scan rate of 50 mV s⁻¹ (versus Ag/AgCl). ^c Optical bandgap calculated from absorption edge of the polymer film: $E_g = 1240/\lambda_{\text{onset}}$. ^d The HOMO energy levels were calculated from $E_{1/2}^{\text{ox}}$ values of CV diagrams and were referenced to ferrocene (4.8 eV relative to vacuum energy level; $E_{\text{onset}} = 0.34$ V; $E_{1/2} = 0.41$ V in acetonitrile). $E_{\text{HOMO}} = -[(E_{1/2}^{\text{ox}} - E_{1/2}^{\text{Fc}}) - 4.8]$ (eV); $E_{\text{LUMO}} = E_{\text{HOMO}} - E_g$.

Table 2 Optical and electrochemical properties of two polymers for calculation of colouration efficiency

Polymers	λ_{\max}^a (nm)	$\Delta T\%$	Response time ^b		ΔOD^c	Q_d^d (mC cm ⁻²)	CE ^e (cm ² C ⁻¹)
			t_c (s)	t_b (s)			
p-2,6-TPAANT							
	770	87 ± 1	1.2 ± 0.02	0.96 ± 0.02	0.881	3.97	222
p-2,6-TPACNANT							
	800	86 ± 2	1.35 ± 0.03	0.92 ± 0.03	0.874	4.19	200

^a Wavelength of absorption maximum. ^b Time for 95% of the full-transmittance change. ^c Optical density change (ΔOD) = $\log[T_{\text{bleached}}/T_{\text{coloured}}]$, where T_{coloured} and T_{bleached} are the maximum transmittance in the oxidized and neutral states, respectively. ^d Q_d is ejected charge, determined from the *in situ* experiments. ^e Colouration efficiency (CE) = $\Delta OD/Q$.

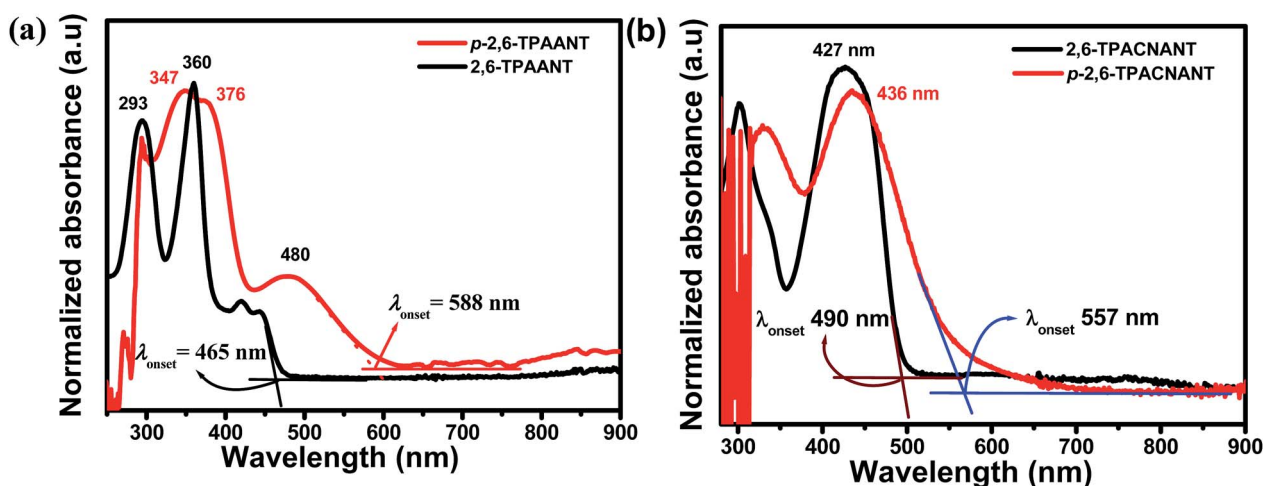


Fig. 3 UV-vis absorption spectra of 2,6-TPAANT and 2,6-TPACNANT in DCM and the p-2,6-TPAANT and p-2,6-TPACNANT films on ITO-glass.

monomers, was observed, which implied the presence of higher conjugations in polymers.

Electrochemistry of the polymer films

Using the monomer solutions at fixed concentrations, the film thickness was easily modulated by controlling the CV scan number in the electropolymerization process (Fig. S1†). Upon washing with DCM, ethanol and acetone, the unreacted

monomer and oligomeric species were removed, and a compact brick red or orange film was formed on the surface of the ITO electrode. Electrochemical behaviour of the electrodeposited films of **p-2,6-TPAANT** and **p-2,6-TPACNANT** was investigated by cyclic voltammetry in the $\text{Bu}_4\text{NClO}_4/\text{CH}_3\text{CN}$ solution (Fig. 2). The half-wave potentials ($E_{1/2}$) of **p-2,6-TPAANT** and **p-2,6-TPACNANT** were read at 0.97 V and 1.01 V, respectively. Both polymers revealed only one oxidation peak although, two

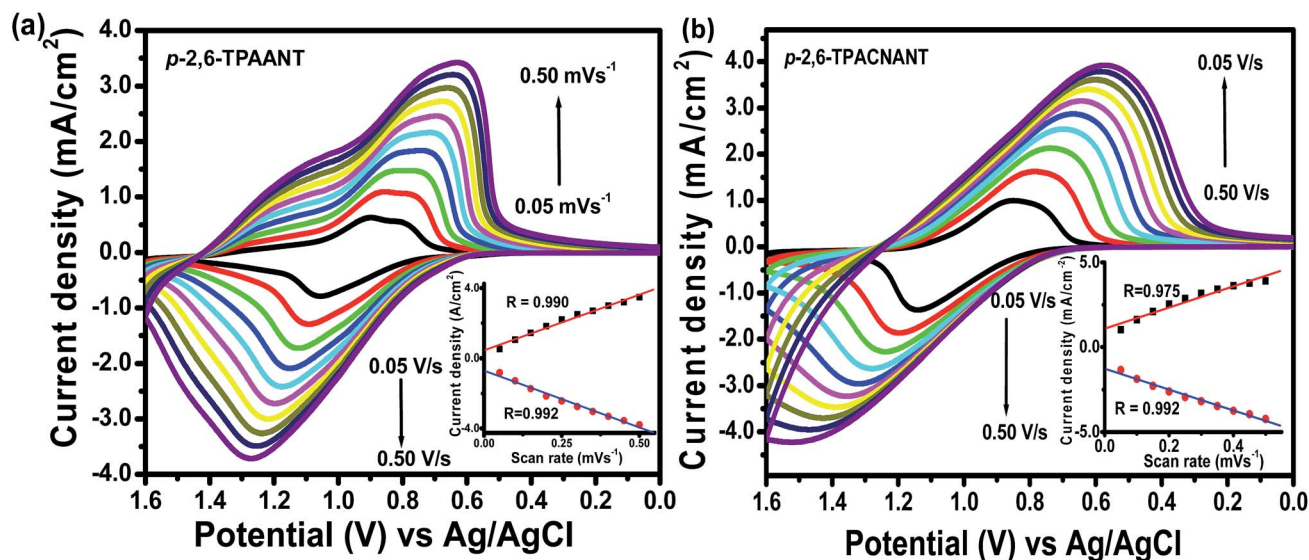


Fig. 4 Scan rate dependence p-2,6-TPAANT and p-2,6-TPACNANT films on ITO-coated glass slide in 0.1 M $\text{Bu}_4\text{NClO}_4/\text{CH}_3\text{CN}$ at different scan rates between 0.05 and 0.50 V s^{-1} .

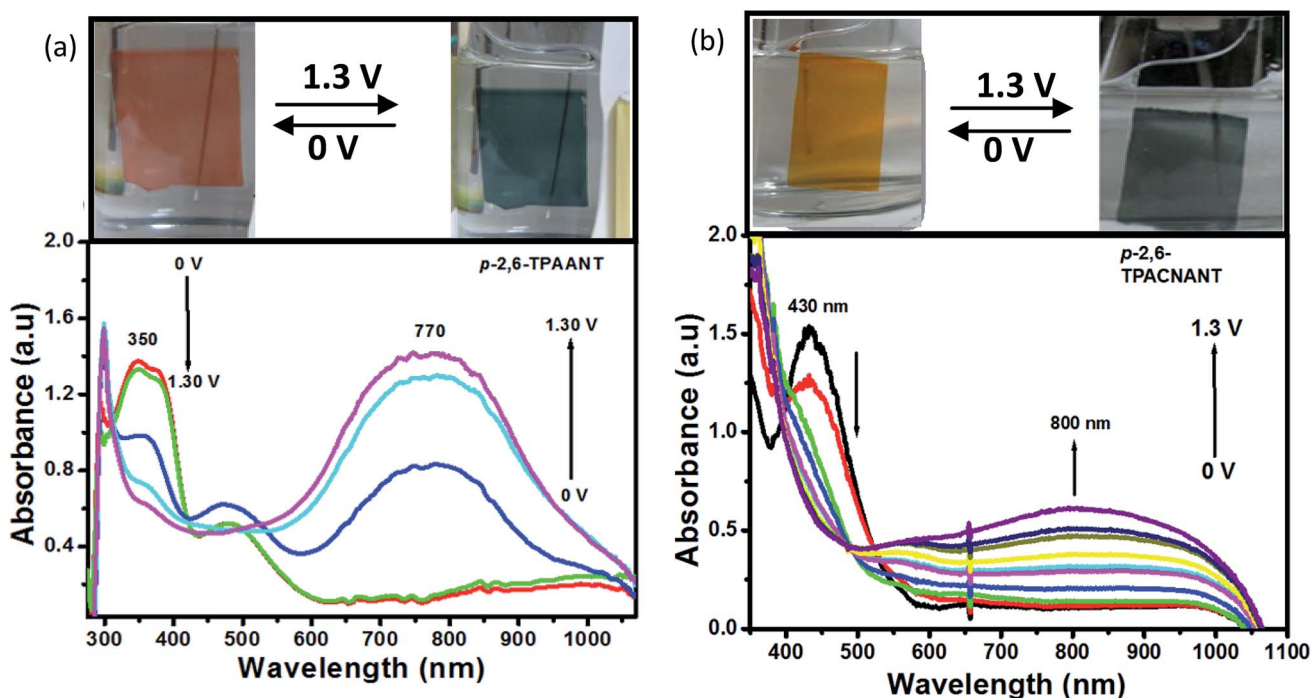


Fig. 5 Absorption spectra of (a) p-2,6-TPAANT (b) p-2,6-TPACNANT films on ITO-coated glass in 0.1 M $\text{Bu}_4\text{ClO}_4/\text{CH}_3\text{CN}$ at different applied potentials (0 to 1.3 V).

oxidation processes of the TBP moiety were expected. It might be a fact that the oxidation wave of the TPB unit merged and became undistinguishable in the CV diagram.

The quantitative details of the polymers are summarized in Table 1. The energy levels of the highest occupied molecular orbital (HOMO) and the lowest unoccupied molecular orbital (LUMO) energy levels of polymers were estimated from the E_{onset} and $E_{1/2}^{\text{ox}}$ values with reference to the CV diagram of ferrocene (Fig. S3,† and its $E_{1/2}^{\text{Fc}} = 0.41$ eV). Assuming that the HOMO energy level for the ferrocene/ferrocenium (Fc/Fc^+) standard was 4.80 eV with respect to the zero vacuum level, the HOMO levels for **p-2,6-TPAANT** and **p-2,6-TPACNANT** were found to be 5.36 and 5.40 eV, respectively. From the absorption spectra (Fig. 3) of the polymers, optical band gap (E_g) were calculated 2.11 eV for **p-2,6-TPAANT** and 2.23 eV for **p-2,6-TPACNANT**. Taking the values of band gap and the HOMO of respective polymers, LUMOs were estimated to 3.25 eV for **p-2,6-TPAANT** and 3.17 eV for **p-2,6-TPACNANT**. The electrochemical behaviour of the polymer **p-2,6-TPAANT** and **p-2,6-TPACNANT** films at different scan rates between 0.05 V s^{-1} and 0.50 V s^{-1} in $0.1 \text{ M Bu}_4\text{NClO}_4/\text{CH}_3\text{CN}$ reveal the gradual shift of the potential with increased current densities (Fig. 4). A linear dependence of the peak current as a function of scan rates indicated that the electrochemical processes of these polymers were reversible and not diffusion limited.

Spectroelectrochemical and electrochromic properties of polymers. To understand its electronic structure and optical behaviour during electro-oxidation, the spectral changes (Fig. 5a and b) of the **p-2,6-TPAANT** and **p-2,6-TPACNANT** of electro-deposited polymeric films on ITO electrode were performed upon applying the different potentials from 0 to 1.3 V (*versus* Ag/AgCl) in $0.1 \text{ M Bu}_4\text{NClO}_4/\text{CH}_3\text{CN}$ monomer free electrolyte solution. In the neutral state, the polymer **p-2,6-TPAANT** showed strong absorption at wavelengths around 350 nm, characteristic of the triphenylamine $\pi-\pi^*$ transitions unit in the polymer backbone. When the potential was steadily increased from 0 to 1.3 V, the absorption around 350 nm corresponding to the neutral state decreased with concomitant growth of a broad band at around an absorption maximum 770 nm. The new band (770 nm) corresponded to the formation of stable dication by full oxidation of the electro-cross-linking TPA segments in the electropolymer film. In the meantime, the colour of the film changed from brick red to dark blue. Fig. 3b, **p-2,6-TPACNANT** demonstrates the strong absorption in the neutral state at wavelengths around 436 nm, assigned to the $\pi-\pi^*$ transitions unit of the polymer backbone containing triphenylamine. When the potential was steadily increased from 0 to 1.3 V, the absorption around 436 nm corresponding to the neutral state was depleted, with an appearance of a new broad band centred at 800 nm with the extended tail in the near-infrared region. Upon oxidation, the radical cations (polarons) or dications (bipolarons)^{18g} were formed and the absorption was transferred

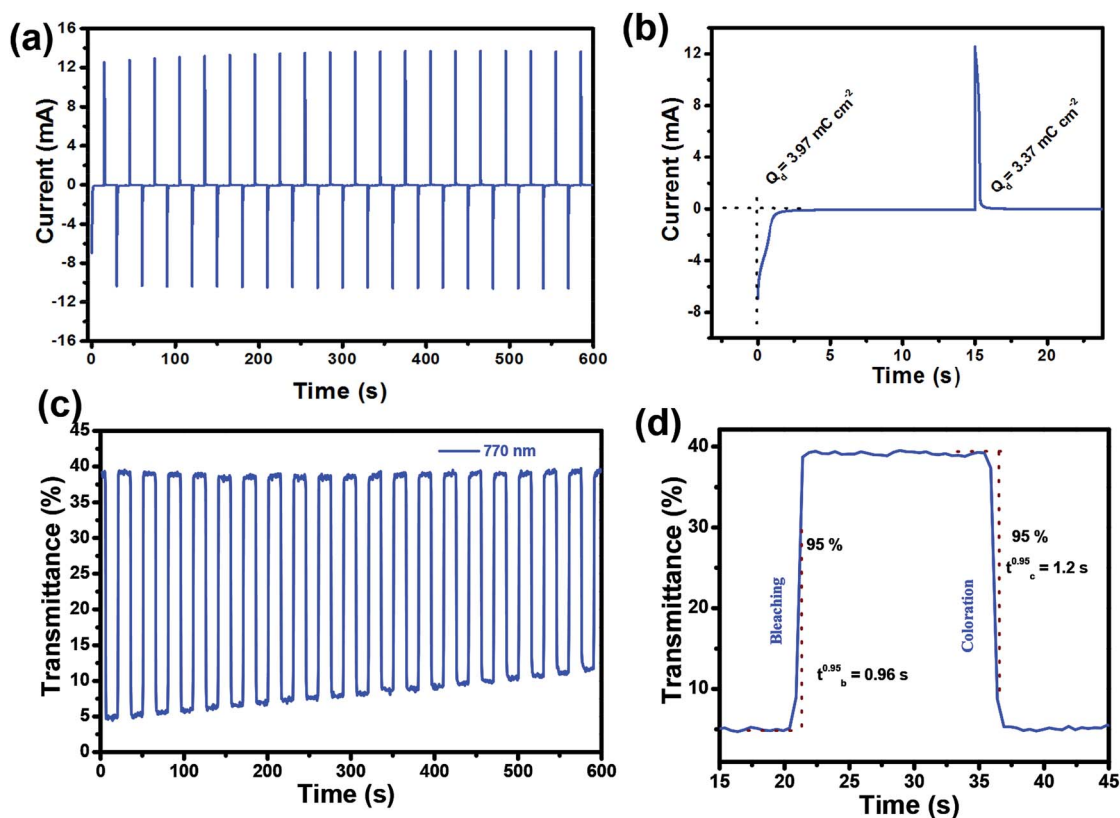


Fig. 6 The simultaneous monitoring of (a and b) switching current (c and d) transmittance for **p-2,6-TPAANT** on the ITO-glass slide (coated area 0.98 cm^2) (in CH_3CN with $0.1 \text{ M Bu}_4\text{NClO}_4$ as the supporting electrolyte) monitored at 770 nm, when it was switched between its neutral (0 V *vs.* Ag/AgCl) and oxidized (1.30 V *vs.* Ag/AgCl) states at 15 s intervals.

into the NIR region with the depletion of ground state π - π^* transition in the visible region. Simultaneously, the colour of the film changed from orange to dark blue. More importantly, these colour changes of solid film were highly reversible in nature upon oxidation-reduction and it occurred without any special protection such as oxygen and humidity. Indeed, these colour changes were visualized readily by the naked eye.

The electrochromic response of both the polymers **p-2,6-TPAANT** and **p-2,6-TPACNANT** were further investigated by double-potential-step chrono-amperometry and chrono-absorptometry (Fig. 6 and 7). The percent transmittance, changes (%*T*) at a certain wavelength (λ_{max}), was monitored as a function of time by switching between potentials from 0 to 1.3 V *versus* Ag/AgCl with a pulse width of 15 s. Switching data for the electrodeposited film of **p-2,6-TPAANT** are presented in Fig. 6. The response time monitored at 770 nm was calculated at 95% of the full transmittance change for the polymer **p-2,6-TPAANT**. The time required for 95% full transmittance changes were 1.2 s for the colouration step and 0.96 s for the bleaching step. The optical contrast ratio (ΔT , % *i.e.* the percentage of transmittance change) of 87% at 770 nm was achieved by taking the value of colouration transmittance 5.2% (the turn-ON state) and the bleaching transmittance of 39.5% (the turn-OFF state) at the first potential switching step. Colouration efficiency (η) was a useful parameter for determining the quality of

electrochromic materials. The relationship between the optical density change (ΔOD) and the injected/ejected electronic charge (Q_d) was presented by the following equation

$$\eta = \frac{\Delta OD}{Q_d} = \log \frac{T_b}{T_c} / Q_d$$

Where ΔOD was the optical absorbance change, and ' Q_d ' (mC cm^{-2}) was the inject/ejected charge during a redox step. A higher ' η ' value was observed when the electrochromic materials had a large optical change and/or low electronic charge. On the basis of this equation, the CE values of **p-2,6-TPAANT** were calculated as $222 \text{ cm}^2 \text{ C}^{-1}$ (at 770 nm). However, the polymer film displayed a larger loss of optical contrast after 20 switching cycles between the neutral and the oxidized states (from 87% to 71%).

For the polymer **p-2,6-TPACNANT**, the switching stability λ_{max} at 800 nm was investigated by monitoring the optical contrast of the thin film upon repeated potential steps between 0 and 1.30 V with a pulse width of 15 s, (Fig. 7). In this case, a response time was required for 95% full-transmittance change of 1.35 s for the colouration step and 0.92 s for the bleaching step. In addition, the optical contrast measured as ΔT recorded in neutral and oxidized forms were found to be 86% at 800 nm (10.5% *T* in the turn-ON state and 78.5% *T* in the turn-OFF state). However, the polymer film displayed a larger loss of

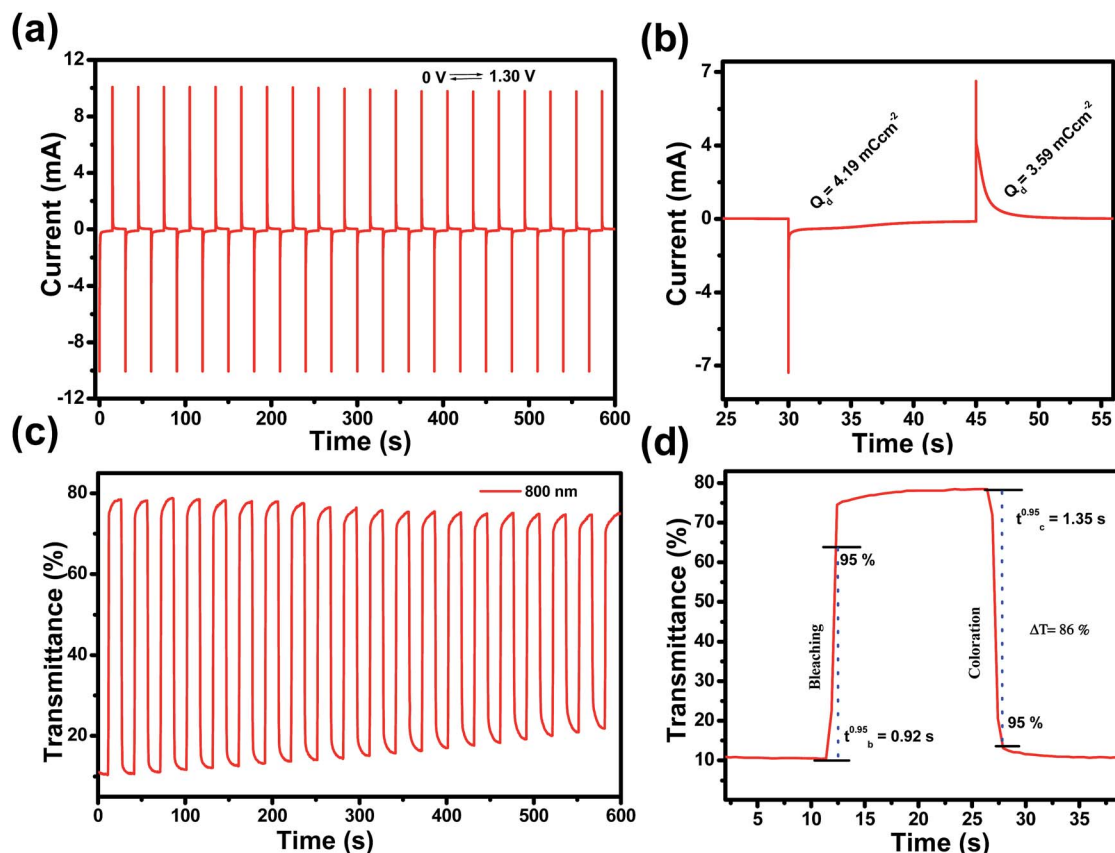


Fig. 7 The simultaneous monitoring of (a and b) switching current (c and d) transmittance for **p-2,6-TPACNANT** on the ITO-glass slide (coated area 1.1 cm^2) (in CH_3CN with $0.1 \text{ M Bu}_4\text{NClO}_4$ as the supporting electrolyte) monitored at 800 nm, when it was switched between its neutral (0 V *vs.* Ag/AgCl) and oxidized (1.30 V *vs.* Ag/AgCl) states at 15 s intervals.

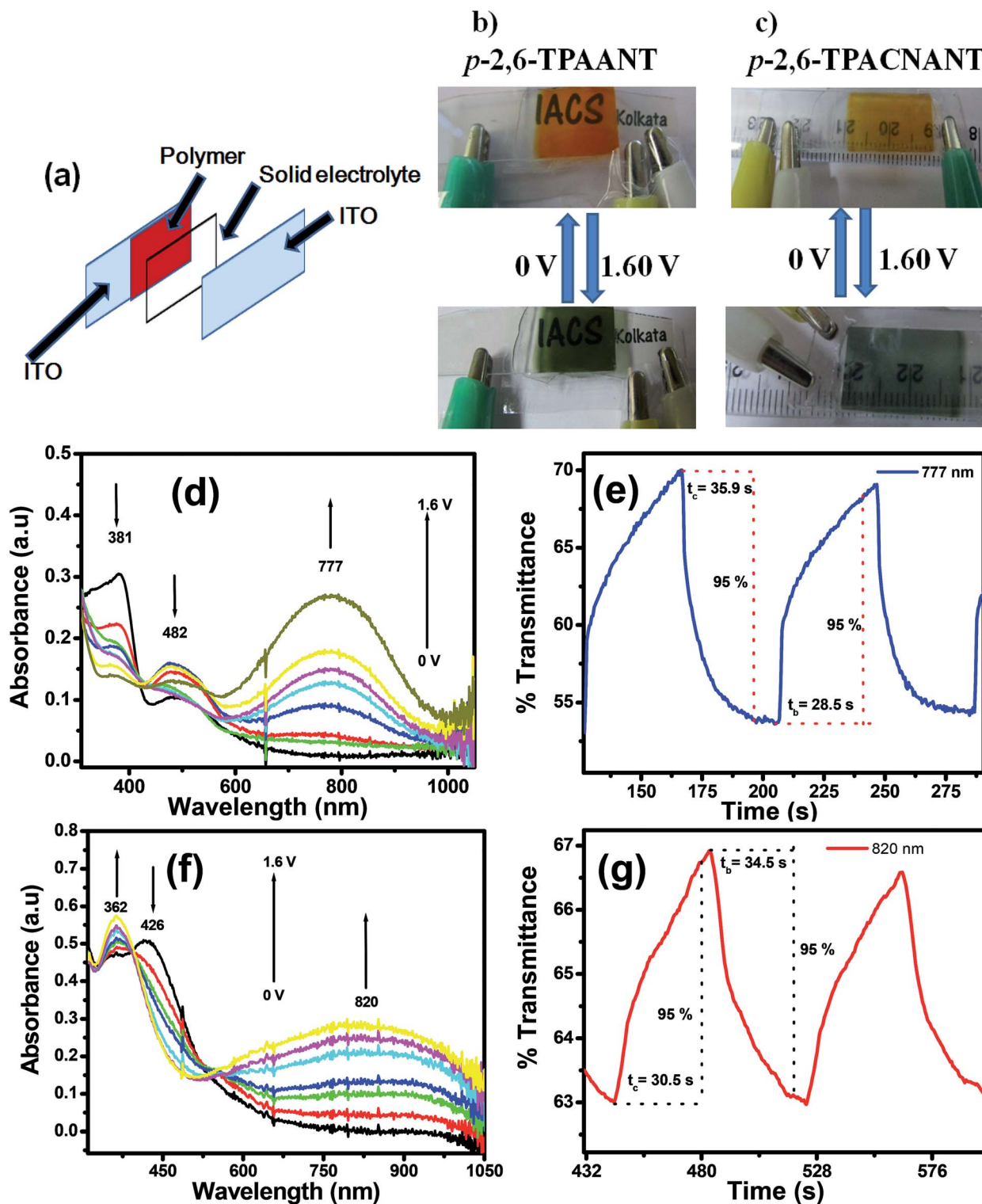


Fig. 8 (a) Schematic illustration of the structure of the electrochromic devices (b) and (c) are the photos of the sandwich-type ITO-coated glass electrochromic cell, using p-2,6-TPAANT and p-2,6-TPACNANT as the active layer. Electrochromic device (ECD) spectra and corresponding switching behaviour (d), (e) for p-2,6-TPAANT and (f), (g) for p-2,6-TPACNANT.

optical contrast after 20 switching cycles between the neutral and the second oxidized states (from 87% to 71%). The CE values of p-2,6-TPACNANT were calculated to be $200 \text{ cm}^2 \text{ C}^{-1}$ at 800 nm by chronoamperometry.

Electrochromic devices fabrication

To demonstrate the application of these electrodeposited polymeric films, an electrochromic device was constructed utilizing a solid state electrolyte containing PMMA and LiClO_4 , as

plasticized with propylene carbonate to form a highly transparent and conductive gel. The polymer films were electro-deposited onto ITO-coated glass, thoroughly rinsed with DCM, CH₃OH and CH₃COCH₃ three times and finally dried. The gel electrolyte was spread on the polymer-coated side of the electrode and kept in normal air. After that, it was put in an oven for 1 h at 60 °C and the electrodes were sandwiched with another ITO. Finally, an epoxy resin was used to seal the device. A schematic diagram of the electrochromic cell is shown in Fig. 8. Upon applying voltage from 0 V to 1.6 V, the colour change occurred from brick red to a dark blue for **p-2,6-TPAANT** and yellow to dark blue for **p-2,6-TPACNANT**. When the potential was subsequently set back at 0 V, the polymer film changed back to its initial colour. Reverse potential change of the initial colour is faster than the oxidized colour. Reversible colour changes were perceived by the naked eye several times.

Conclusions

To summarize, two electrochromic film **p-2,6-TPAANT** and **p-2,6-TPACNANT** were prepared through oxidative electropolymerization of the TPA-substituted anthracene derivatives in Bu₄NClO₄/DCM. However, no polymer film was deposited on the ITO electrode surface using the mono-TPA substituted derivative of anthracene (**2-TPACNANT**). The electro-deposited films exhibited reversible electrochemical oxidation accompanied by distinct colour changes observed by naked eye. The film thickness was easily tuned by controlling the CV scan number. The adherent film revealed the low-voltage controlled electrochromism with a significant optical contrast ratio (86% to 87% at 770 nm and 800 nm), fast response time (1.2 s and 1.3 s for the colouration step and 0.96 s and 0.92 s for the bleaching step), and high colouration efficiency (CE = 222 cm² C⁻¹ and 200 cm² C⁻¹). These characteristics suggest that these electro-deposited polymers are promising materials for use in optoelectronics applications. Studies on further expanding its spectral response range and improving its stability are currently going on in this laboratory.

Acknowledgements

Dr Malik acknowledges CSIR, INDIA (project no. 02(0161)/13/EMR-II) for the partial financial support of this work. S. Mondal is thankful to CSIR, New Delhi, India for the fellowship.

References

- 1 P. R. Somani and S. Radhakrishnan, *Mater. Chem. Phys.*, 2002, **77**, 117–133.
- 2 P. M. Beaujuge and J. R. Reynolds, *Chem. Rev.*, 2010, **110**, 268–320.
- 3 W. A. Gazotti, G. Casalbore-Miceli, A. Geri, A. Berlin and M. A. de Paoli, *Adv. Mater.*, 1998, **10**, 1522–1525.
- 4 H. Liu and R. M. Crooks, *Anal. Chem.*, 2012, **84**, 2528–2532.
- 5 R. J. Mortimer, A. L. Dyer and J. R. Reynolds, *Displays*, 2006, **27**, 2–18.
- 6 J. Matsui, R. Kikuchi and T. Miyashita, *J. Am. Chem. Soc.*, 2014, **136**, 842–845.
- 7 B. A. Korgel, *Nature*, 2013, **500**, 278–279.
- 8 S. V. Vasilyeva, P. M. Beaujuge, S. Wang, J. E. Babiarz, V. W. Ballarotto and J. R. Reynolds, *ACS Appl. Mater. Interfaces*, 2011, **3**, 1022–1032.
- 9 C. J. Chen, H.-J. Yen, Y.-C. Hu and G.-S. Liou, *J. Mater. Chem. C*, 2013, **1**, 7623–7634.
- 10 A. Azens and C. Granqvist, *J. Solid State Electrochem.*, 2003, **7**, 64–68.
- 11 C. G. Granqvist, A. Azens, A. Hjelm, L. Kullman, G. A. Niklasson, D. Rönnow, M. S. Mattsso, M. Veszele and G. Vaivars, *Sol. Energy*, 1998, **63**, 199–216.
- 12 J. Z. Chen, W. Y. Ko, Y. C. Yen, P. H. Chen and K. J. Lin, *ACS Nano*, 2012, **6**, 6633–6639.
- 13 C. Pozo-Gonzalo, D. Mecerreyes, J. A. Pomposo, M. Salsamendi, R. Marcilla, H. Grande, R. Vergaz, D. Barrios and J. M. Sánchez-Pena, *Sol. Energy Mater. Sol. Cells*, 2008, **92**, 101–106.
- 14 V. K. Thakur, G. Ding, J. Ma, P. S. Lee and X. Lu, *Adv. Mater.*, 2012, **24**, 4071–4096.
- 15 (a) Y. Y. Song, Z. D. Gao, J. H. Wang, X. H. Xia and R. Lynch, *Adv. Funct. Mater.*, 2011, **21**, 1941–1946; (b) Y. C. Nah, A. Ghicov, D. Kim, S. Berger and P. Schmuki, *J. Am. Chem. Soc.*, 2008, **130**, 16154–16155; (c) C. Liao, F. Chen and J. Kai, *Sol. Energy Mater. Sol. Cells*, 2007, **91**, 1282–1288; (d) G. A. Niklasson and C. G. Granqvist, *J. Mater. Chem.*, 2007, **17**, 127–156; (e) C. Lamsal and N. M. Ravindra, *J. Mater. Sci.*, 2013, **48**, 6341–6351.
- 16 (a) L. Groenendaal, G. Zotti, P.-H. Aubert, S. M. Waybright and J. R. Reynolds, *Adv. Mater.*, 2003, **15**, 855–879; (b) A. A. Argun, P.-H. Aubert, B. C. Thompson, I. Schwendeman, C. L. Gaupp, J. Hwang, N. J. Pinto, D. B. Tanner, A. G. MacDiarmid and J. R. Reynolds, *Chem. Mater.*, 2004, **16**, 4401–4412; (c) G. Sonmez, I. Schwendeman, P. Schottland, K. Zong and J. R. Reynolds, *Macromolecules*, 2003, **36**, 639–647; (d) G. Sonmez, *Chem. Commun.*, 2005, 5251–5259; (e) A. Patra, Y. H. Wijsboom, S. S. Zade, M. Li, Y. Sheynin, G. Leitius and M. Bendikov, *J. Am. Chem. Soc.*, 2008, **130**, 6734–6736; (f) R. M. Walczak, J.-H. Jung, J. S. Cowart Jr and J. R. Reynolds, *Macromolecules*, 2007, **40**, 7777–7785; (g) R. M. Walczak and J. R. Reynolds, *Adv. Mater.*, 2006, **18**, 1121–1131; (h) A. Patra and M. Bendikov, *J. Mater. Chem.*, 2010, **20**, 422–433.
- 17 M. Li, Y. Wei, J. Zheng, D. Zhu and C. Xu, *Org. Electron.*, 2014, **15**, 428–434.
- 18 (a) R. J. Mortimer, *Electrochim. Acta*, 1999, **44**, 2971–2981; (b) Y. Shiota, *J. Mater. Chem.*, 2000, **10**, 1–25; (c) G. Sonmez, C. K. F. Shen, Y. Rubin and F. Wudl, *Angew. Chem., Int. Ed.*, 2004, **43**, 1498–1502; (d) J. Sun, X. Lv, P. Wang, Y. Zhang, Y. Dai, Q. Wu, M. Ouyang and C. Zhang, *J. Mater. Chem. C*, 2014, **2**, 5365–5371; (e) S. H. Hsiao and J.-W. Lin, *Polym. Chem.*, 2014, **5**, 6770–6778; (f) C. Fan, C. Ye, X. Wang, Z. Chen, Y. Zhou, Z. Liang and X. Tao, *Macromolecules*, 2015, **48**, 6465–6473; (g) S.-H. Hsiao and S.-W. Lin, *Polym. Chem.*, 2016, **7**, 198–211; (h) S. H. Hsiao

- and J. Y. Lin, *J. Polym. Sci., Part A: Polym. Chem.*, 2016, **54**, 644–655.
- 19 (a) C. Fan, C. Ye, X. Wang, Z. Chen, Y. Zhou, Z. Liang and X. Tao, *Macromolecules*, 2015, **48**, 6465–6473; (b) D. Qiu, Q. Zhao, X. Bao, K. Liu, H. Wang, Y. Guo, L. Zhang, J. Zeng and H. Wang, *Inorg. Chem. Commun.*, 2011, **14**, 296–299.
- 20 (a) H.-J. Yen, H.-Y. Lin and G.-S. Liou, *Chem. Mater.*, 2011, **23**, 1874–1882; (b) H.-J. Yen, H.-Y. Lin and G.-S. Liou, *J. Mater. Chem.*, 2011, **21**, 6230–6237; (c) H.-J. Yen and G.-S. Liou, *Polym. Chem.*, 2012, **3**, 255–264; (d) H.-J. Yen and G.-S. Liou, *Chem. Commun.*, 2013, **49**, 9797–9799; (e) J. Yen, C.-J. Chen and G.-S. Liou, *Adv. Funct. Mater.*, 2013, **23**, 5307–5316.
- 21 (a) Y.-C. Kung and S.-H. Hsiao, *J. Mater. Chem.*, 2010, **20**, 5481–5492; (b) Y.-C. Kung and S.-H. Hsiao, *J. Mater. Chem.*, 2011, **21**, 1746–1754; (c) S.-H. Hsiao, H.-M. Wang, P.-C. Chang, Y.-R. Kung and T.-M. Lee, *J. Polym. Sci., Part A: Polym. Chem.*, 2013, **51**, 2925–2938; (d) H.-M. Wang and S.-H. Hsiao, *J. Mater. Chem. C*, 2014, **2**, 1553–1564; (e) S.-H. Hsiao, H.-M. Wang and S.-H. Liao, *Polym. Chem.*, 2014, **5**, 2473–2483; (f) H.-M. Wang and S.-H. Hsiao, *J. Polym. Sci., Part A: Polym. Chem.*, 2014, **52**, 272–286; (g) S.-H. Hsiao, P.-C. Chang, H.-M. Wang, Y.-R. Kung and T.-M. Lee, *J. Polym. Sci., Part A: Polym. Chem.*, 2014, **52**, 825–838; (h) H.-M. Wang and S.-H. Hsiao, *J. Polym. Sci., Part A: Polym. Chem.*, 2014, **52**, 1172–1184; (i) S.-H. Hsiao and S.-L. Cheng, *J. Polym. Sci., Part A: Polym. Chem.*, 2015, **53**, 496–510.
- 22 (a) Y. Shirota and H. Kageyama, *Chem. Rev.*, 2007, **107**, 953–1010; (b) C. H. Ku, C. H. Kuo, C. Y. Chen, M. K. Leung and K. H. Hsieh, *J. Mater. Chem.*, 2008, **18**, 1296–1301; (c) Y. K. Fang, C. L. Liu, G. Y. Yang, P. C. Chen and W. C. Chen, *Macromolecules*, 2011, **44**, 2604–2612.
- 23 (a) E. T. Seo, R. F. Nelson, J. M. Fritsch, L. S. Marcoux, D. W. Leedy and R. N. Adams, *J. Am. Chem. Soc.*, 1966, **88**, 3498–3503; (b) R. F. Nelson and R. N. Adams, *J. Am. Chem. Soc.*, 1968, **90**, 3925–3930; (c) S. C. Creason, J. Wheeler and R. F. Nelson, *J. Org. Chem.*, 1972, **37**, 4440–4446.
- 24 (a) D. C. Santra, M. K. Bera, P. K. Sukul and S. Malik, *Chem. – Eur. J.*, 2016, **22**, 2012–2019; (b) O. P. Lee, A. T. Yiu, P. M. Beaujuge, C. H. Woo, T. W. Holcombe, J. E. Millstone, J. D. Douglas, M. S. Chen and J. M. J. Fréchet, *Adv. Mater.*, 2011, **23**, 5359–5363; (c) S. Zeng, L. Yin, C. Ji, X. Jiang, K. Li, Y. Li and Y. Wang, *Chem. Commun.*, 2012, **48**, 10627–10629.